Bioactive Materials 3 (2018) 64–73

Contents lists available at ScienceDirect

Bioactive Materials

journal homepage: http://www.keaipublishing.com/en/journals/bioactive-materials/

Evaluation of photochemistry reaction kinetics to pattern bioactive proteins on hydrogels for biological applications

Taylor B. Dorsey [a, b, c], Alexander Grath [a, b], Annling Wang [b], Cancan Xu [d], Yi Hong [d], Guohao Dai [a, b, c, *]

[a] Department of Biomedical Engineering, Rensselaer Polytechnic Institute, Troy, NY 12180, USA
[b] Center for Biotechnology and Interdisciplinary Studies, Rensselaer Polytechnic Institute, Troy, NY 12180, USA
[c] Department of Bioengineering, Northeastern University, Boston, MA 02115, USA
[d] Department of Bioengineering, University of Texas at Arlington, Arlington, TX 76019, USA

ARTICLE INFO

Article history:
Received 24 March 2017
Accepted 10 May 2017
Available online 13 May 2017

Keywords:
Photo-patterning
Bioactive signals
PEG hydrogels
Click-chemistry

ABSTRACT

Bioactive signals play many important roles on cell function and behavior. In most biological studies, soluble biochemical cues such as growth factors or cytokines are added directly into the media to maintain and/or manipulate cell activities *in vitro*. However, these methods cannot accurately mimic certain *in vivo* biological signaling motifs, which are often immobilized to extracellular matrix and also display spatial gradients that are critical for tissue morphology. Besides biochemical cues, biophysical properties such as substrate stiffness can influence cell behavior but is not easy to manipulate under conventional cell culturing practices. Recent development in photocrosslinkable hydrogels provides new tools that allow precise control of spatial biochemical and biophysical cues for biological applications, but doing so requires a comprehensive study on various hydrogel photochemistry kinetics to allow thorough photocrosslink reaction while maintain protein bioactivities at the same time. In this paper, we studied several photochemistry reactions and evaluate key photochemical parameters, such as photoinitiators and ultra-violet (UV) exposure times, to understand their unique contributions to undesired protein damage and cell death. Our data illustrates the retention of protein function and minimize of cell health during photoreactions requires careful selection of photoinitiator type and concentration, and UV exposure times. We also developed a robust method based on thiol-norbornene chemistry for independent control of hydrogel stiffness and spatial bioactive patterns. Overall, we highlight a class of bioactive hydrogels to stiffness control and site specific immobilized bioactive proteins/peptides for the study of cellular behavior such as cellular attraction, repulsion and stem cell fate.

1. Introduction

The development of bioactive materials is vital for introducing new methods to study and manipulate cell behavior. Currently, the majority of *in vitro* cell studies rely on tissue culture plastic (TCP) as a culture substrate and soluble biochemical cues for regulating cell activities. These methods, however, are unable to accurately display certain signaling motifs found *in vivo* environments, including immobilized growth factors, cell-cell ligand-receptor interactions, and spatially localized signaling. Furthermore, biophysical cues such as tissue stiffness have important roles in cell phenotype [1–3], whereas TCP does not provide physiologically relevant stiffness. To overcome these challenges, bioactive materials are excellent candidates for mimicking tissue stiffness, immobilizing biomolecules, and creating spatially specific biochemical patterns. Specifically tailored hydrogels have been previously successful in influencing cell morphology [4], cell function [5,6] as well as stem cell fate [3].

Abbreviations: UV, ultra-violet; ECM, extracellular matrix; TCP, tissue culture plastic; PEG, polyethylene glycol; PEGDA, polyethylene glycol diacrylate; DMPA, 2-dimethoxy-2-phenylacetophenone; LAP, lithium phenyl-2,4,6-trimethylbenzoylphosphinate; VEGF, vascular endothelial growth factor; EC, endothelial cell; mESC, mouse embryonic stem cell; HUVEC, human umbilical vein endothelial cell.

* Corresponding author. Department of Bioengineering, Northeastern University, Lake Hall 214A, 360 Huntington Avenue, Boston, MA 02115, USA.
E-mail address: g.dai@northeastern.edu (G. Dai).
Peer review under responsibility of KeAi Communications Co., Ltd.

http://dx.doi.org/10.1016/j.bioactmat.2017.05.005

Hydrogels are commonly used as cell scaffolds due to their biophysical and biochemical commonalities with the extracellular matrix (ECM) [7,8]. Natural polymers, such as collagen or fibrinogen, are common choices for scaffolds as they are biocompatible and found in many tissues of the body, but they lack the easily targeted chemical moieties for bioconjugation purposes. Synthetic hydrogels are advantageous for the manipulation of both stiffness and bioactive molecule attachment. In particular, polyethylene glycol (PEG) is a biologically inert synthetic polymer commonly utilized as a blank slate for cell scaffolds [9,10]. Photopolymerization can be used for PEG hydrogel formation and bioconjugation [10]. Photochemistry requires a photoinitiator and ultra-violet (UV) light exposure to initiate and propagate the reaction. When photoinitiators are introduced to UV light, chemical bonds break to form radicals. Theses radicals are critical for the reaction initiation but can also negatively affect proteins or cells that are present [11]. Two common photoinitiators used in bio-related PEG crosslinking include 2-dimethoxy-2-phenylacetophenone (DMPA) and lithium phenyl-2,4,6-trimethylbenzoylphosphinate (LAP) [12,13]. Specifically, DMPA has been often used in combination with acrylate PEG chemistry [10,12]. LAP has recently reported in studies utilizing thiol-ene reactions [13].

Additionally, there are different photo-reactive chemistries employed for PEG hydrogel synthesis. Acrylate hydrogels entail PEG-diacrylate (PEGDA) monomers undergoing acrylate-acrylate chain growth polymerization resulting in randomly crosslinked networks [12,13]. Another approach is thiol-ene based chemistry [14,15]. Differently, thiol-ene reactions create uniform crosslinks via step growth polymerization and therefore require two reactants: PEG-dithiol monomers and multi-arm PEG containing an “ene” carbon double bond functional group. Thiol-ene, also known as click reactions, can be employed with a variety of “ene” functional groups. Moreover, these functional groups exhibit different reaction kinetics [16] and therefore offer several choices depend on the specific requirement of the applications.

In this study, we investigated how photoinitiator type and concentration influences these photochemistry kinetics, retention of protein bioactivity, and cell viability across a range of UV exposure times. Additionally, we explore both acrylate and thiol-ene PEG hydrogel substrates for stiffness manipulation and surface protein patterning. Finally, we created bioactive hydrogels with vascular endothelial growth factor (VEGF) and ephrinB2 demonstrating its impact on endothelial cell (EC) behavior.

2. Material and methods

2.1. Photoinitiator stock solutions

DMPA (Sigma Aldrich) was dissolved at a concentration of 300 mg/mL in N-Vinylpyrrolidone (NVP, Sigma Aldrich). The LAP was synthesized according to [13]. LAP stock solution was made at a 25 mg/mL in phosphate buffered saline solution. Solutions were passed through 0.22 μm filer for sterilization. Stock solutions were protected from the light with aluminum foil and stored at 4 °C.

2.2. Thiol-ene reaction kinetics

A free thiol colorimetric detection assay, Ellman's Reagent (Thermo Sci.), was used to measure thiol-ene reaction kinetics. In short, the peptide, Arginine-Glycine-Aspartic acid (RGD), was purchased with an additional cysteine residue at the terminus to provide a free thiol for bioconjugation (RGDC, American Peptide). Reduced peptide aliquots were stored in −20 °C to maintain free thiols over time (Supplemental Fig. S1). RGDC was allowed to react with an 8-arm PEG norbornene (JenKem Tech, 20 KDa) at a one to eight molar ratio of norbornene to thiol. The reaction was measured with Ellman's assay after various UV light wavelengths (365 nm or 390 nm) and exposure times, ranging from 10 to 60 s. The amount of free thiols present was calculated and analyzed as inversely proportional to the percentage of reaction that has occurred. Thiol-ene kinetics are reported as a time course and free thiols present are compared to the amount of thiols measured prior to the reaction starts.

2.3. Lysozyme bioactivity assay

To evaluate the bioactivity of proteins after photoreactions, an assay was developed using lysozyme as a model protein. In short, lysozyme (Sigma Aldrich) was exposed to different photoinitiator concentrations and UV light times. For a negative control, lysozyme was boiled for 10 min at 90 °C. Untreated lysozyme served as a positive control. Next, treated lysozyme solutions (1 mg/ml) were added to an overnight *E. coli* culture and incubated for 4 h at room temperature. Solutions were centrifuged and the supernatant was collected for analysis. Bradford assay (Bio-Rad) was used to measure bacteria lysate collected from each treatment group. As expected, the supernatant collected from incubated boiled lysozyme measured no additional protein in the solution; on the other hand, untreated lysozyme measured high concentrations of proteins from the successfully lysed bacteria. Bioactivity is reported as a percentage calculated from the positive control of the assay.

2.4. Cell culture and hydrogel seeding

Mouse embryonic stem cells (mESC) were cultured in 37 °C in 5% CO_2 maintained on 0.1% gelatin coated dishes with ESGRO complete defined serum-free medium (Stem Cell Technologies) with a selective GSK3beta inhibiter. Media was replaced every two days and routinely passaged. For hydrogel seeding, mESCs were added at a cell density of 200,000 cells/cm^2 to various stiffness acrylate hydrogels. Human umbilical cord venous endothelial cells (HUVECs, Lonza) were cultured in 37 °C in 5% CO_2 on 0.1% gelatin coated dishes with Endothelial Cell Growth Medium-2 (EGM-2, Lonza). Media is replaced every two days and passaged regularly. HUVECs were seeded onto patterned hydrogels at a cell density of 70,000 cells/cm^2. HUVECs seeded onto VEGF immobilized hydrogels were cultured with EGM-2 without growth factors.

2.5. Cell viability measurement

To investigate the health of cells that were present during a photoreaction, a photoinitiator was introduced to a cell suspension of HUVECs and exposed to UV light for a specific amount of time. After treatment, HUVECs were seeded into a 96 well plate. After 4 h, cell viability was evaluated using live (calcein AM) dead (ethidium homodimer-1) staining following kit instructions (Thermo Fisher Scientific). As a positive control, HUVECs with no photoinitiator or UV exposure were also seeded and imaged. Additionally, solvent NVP, used in DMPA but not LAP stock solution, was tested to determine its contribution to cell viability (Supplemental Fig. S2). Images were analyzed with ImageJ software to calculate percent cell viability.

2.6. PEG-diacrylate and thiol-ene hydrogel synthesis

Acrylate-acrylate hydrogels were synthesized using polyethylene glycol diacrylate monomers (PEGDA, Laysan Bio, 3.4 kDa). Thiol-ene hydrogels were synthesized by a reaction between PEG-dithiol (Laysan Bio, 3.4 kDa) and 8-arm PEG norbornene (JenKem

Tech, 20 KDa) at an eight to one molar ratio. Precursor solutions were created at a 10% weight/volume in phosphate buffer saline (PBS) with 2 mM of LAP, unless otherwise stated. Gel solutions were passed through a 0.22 μm filer for sterilization. Additionally, fibronectin (60 μg/ml) was added into the precursor solution to improve cell attachment to the hydrogel. After thoroughly mixed, solutions were pipetted into a 0.5 mm thick mold and exposed to UV light (365 nm, 3.4 mW/cm^2) for 2 min, unless otherwise stated. Biopsy punches were used to cut hydrogels into appropriate sized samples and placed into well plates for imaging or cell seeding.

2.7. Hydrogel rheological measurements

Rheology was used to determine the storage modulus of different PEG hydrogels compositions. Acrylate PEG hydrogels were photopolymerized with 11.7 mM of DMPA and UV for two min. 8-arm norbornene PEG hydrogels were each mixed with PEG-dithiol at a 1:8 M ratio with 2 mM of LAP and exposed to UV light for two min. Each hydrogel sample (8 mm diameter, 0.5 mm thickness) was placed into the AR-G2 rheometer (TA Instruments). The parallel plate geometry (8 mm diameter) was lowered until making contact with the surface of the gel (0.5 mm gap distance). Time sweeps were performed at 0.1% strain and 0.1 Hz frequency at 37 °C. Independent hydrogel samples were run as replicates for each composition.

2.8. Protein immobilization and patterning

PEG hydrogel surfaces were modified with thiolated-proteins or peptides via thiol-ene reactions. To introduce thiol group to the protein, proteins were reacted with 2-iminothiolane HCl (Traut's Reagent, Thermo Scientific) following the manufacturer's protocol. NHS-ester fluorescent tags (Dylight488 or Dylight594, Invitrogen) were also reacted with proteins/peptides for pattern visualization. Acrylate-acrylate and thiol-ene PEG hydrogels were photopolymerized, using the method described in the previous section. Next, reduced thiolated proteins or peptides were evenly pipetted across the surface of the hydrogel. For patterning, a photomask was placed directly onto the hydrogel surface. Hydrogels underwent a second round of UV exposure, for 30 s, unless otherwise stated. Hydrogels were placed into well plates for imaging or cell seeding. All hydrogels were washed in phosphate buffer saline (PBS) overnight prior to imaging or cell seeding.

3. Results and discussion

3.1. Thiol-ene reaction kinetics

To select an appropriate functional group for PEG thiol-ene reactions, we explored different “ene” functionalized PEG monomers (Fig. 1a) and observed their reaction kinetics with a thiolated peptide, RGDC (Fig. 1b). Comprising exactly one thiol, RGDC was reacted with a 1:1 functional group of norbornene, maleimide or acrylate functionalized PEG (Fig. 1a). Our results indicated that thiol-norbornene has the quickest reaction speed and best reaction completeness: all thiols were reacted in less than 1 min (~30 s) of UV exposure (Fig. 1c). In comparison, thiol-acrylate reaction is significantly slower: 50% of the thiol is still un-reacted even after 4 min of UV exposure. Thiol-maleimide reaction speed is fast in the beginning but less efficient afterwards with 40% of thiol remains unchanged during the 1–4 min UV exposure time. Moreover, we observed an exponential decay relationship between unreacted free thiols and UV exposure within 30 s (Fig. 1d). Moving forward, thiol-ene reactions were carried out with norbornene functional PEG, as the monomer provides fast and efficient reactions, important features when working with cell encapsulation and/or protein conjugation.

Next, we evaluated photoinitiator type, concentration and UV wavelength contributions to the efficiency of norbornene thiol-ene reactions. LAP initiation resulted in fast reaction kinetics across a range of molar concentrations, with the lowest successful concentration of 0.5 mM (Fig. 1e). On the other hand, DMPA initiated reactions showed slower kinetics and only converted about half of the free thiols after 1 min of UV exposure (Fig. 1f). Furthermore, increases in DMPA concentration failed to increase efficiency.

Next, we tested different UV wavelengths, 365 nm and 390 nm, to examine if either provided better kinetics for each photoinitiator. LAP was able to initiate the reaction similarly using either UV wavelength (Fig. 1g). On the other hand, DMPA was able to initiate the reaction when exposed to 365 nm wavelength but not 390 nm (Fig. 1h). These results illustrate LAP is an excellent photoinitiator for thiol-ene based photochemistries; LAP reactions require shorter UV times and minimal LAP concentrations. DMPA initiated reactions are not appropriate for thiol-ene reactions when speed or high efficiency is desired.

3.2. Photochemistry parameters effect protein bioactivity and cell viability

To examine how photochemistry parameters effect protein bioactivity, we evaluated LAP and DMPA and observed the detrimental effects on lysozyme functions. Comparing the photoinitiators at the same molar concentration, DMPA provided higher activity across all UV times tested. At 4 min of UV light, LAP decreased protein activity to about 40%, whereas DMPA showed no degradation of lysozyme function (Fig. 2a). Additionally, we noticed the concentration of LAP drastically influenced protein function; however, changes in DMPA concentration did not (Fig. 2b). For example, LAP at concentrations greater than 2 mM saw a large reduction in protein function at 30 s of UV exposure, and prolonged UV exposure continued to damage lysozyme (Fig. 2c). Whereas DMPA at different concentrations resulted in varied but overall high bioactivity across tested UV exposure (Fig. 2d). Overall, these results suggest DMPA is a superior photoinitiator for maintaining bioactivity of proteins for high photoinitiator concentrations and long UV exposure times. LAP is still a viable photoinitiator choice for bioconjugation purposes but has a significantly smaller working range in both molar concentration and UV exposure time.

To validate how photochemistry parameters effect cell viability, we employed live dead staining on HUVECs after different treatments of photoinitiators and UV exposures. As a general trend, we observed that cell viability decreases with increases in photoinitiator concentration and/or UV exposure times. At the same molar concentration, LAP provided a higher percentage of live cells at 1 min and 2 min of UV exposure compared to DMPA (Fig. 3a). LAP concentrations tested coupled with 1 min of UV exposure all retained high percentage of viability, but prolonged UV exposure drastically diminished percent of live cells (Fig. 3b). On the other hand, DMPA treatment groups experienced potency with changes in photoinitiator concentration but not as sensitive to UV exposure times (Fig. 3c). In particular, concentrations of 2 mM, 11.7 mM, and 23.4 mM of DMPA with 1 min UV resulted in 80%, 40%, and less than 10% cell viability, respectively (Fig. 3c). In summary, the presence of LAP or DMPA with exposure to UV light can negatively affect the health of cells. When performing photochemistry in the presence of cells, such as for cell encapsulation protocols, UV exposure is an important parameter to minimize when initiating the reaction with LAP whereas photoinitiator concentration is critical to minimize when using DMPA.

In summary, both types of photoinitiators can be successfully

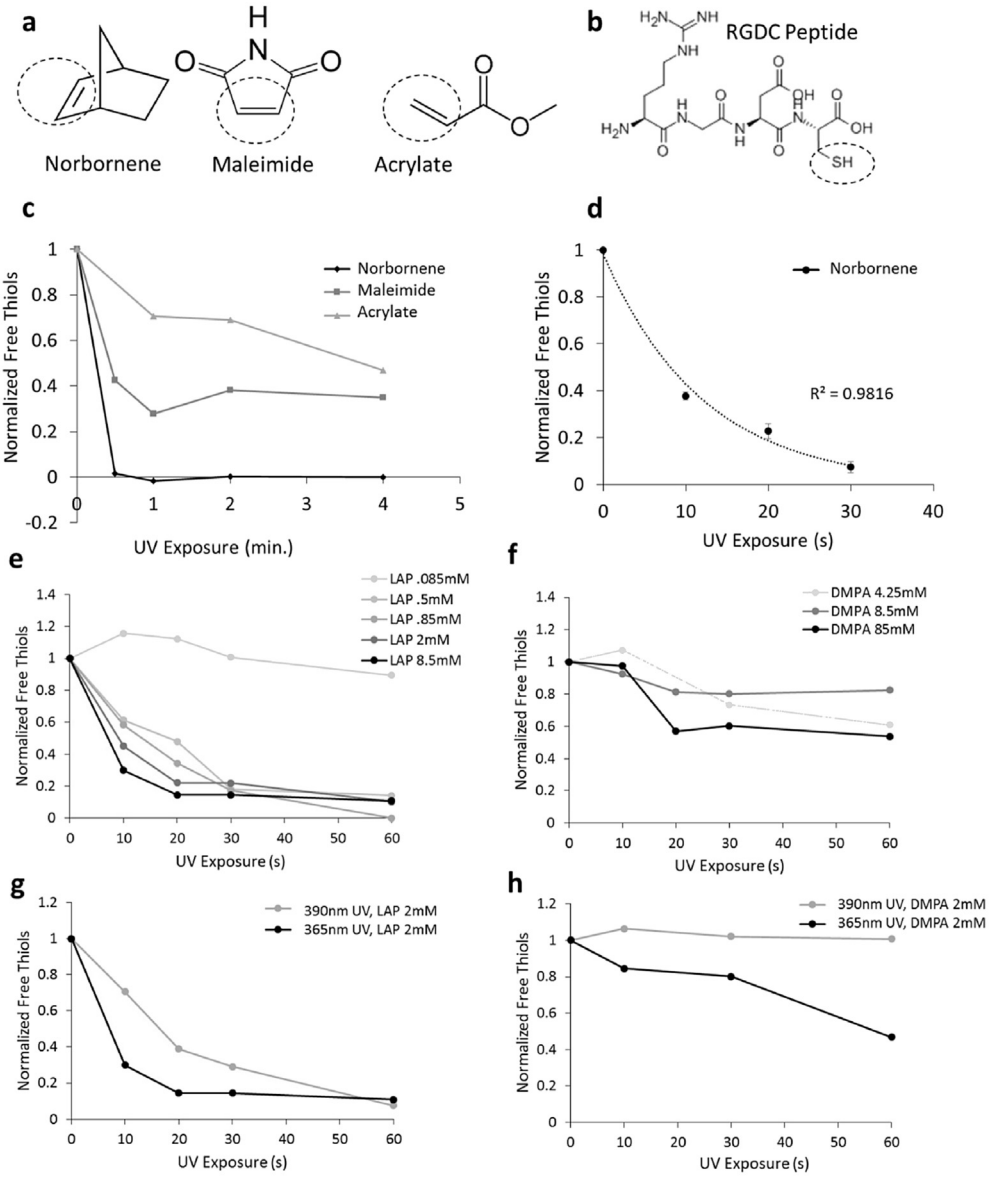

Fig. 1. Reaction kinetics of thiol-ene photo-reactions. (**a**) Tested PEG functional end "ene" groups for thiol-ene reactions, norbornene, maleimide and acrylate. Dashed circles indicate "ene" reaction moiety. (**b**) RGDC peptide as the thiol functional for thiol-ene reactions. Dashed circle indicates thiol moiety. (**c**) Reaction kinetics of different end group PEGs over four minutes of UV exposure. (**d**) Norbornene functionalized multi-arm PEG reaction with RGDC over 30 s of UV exposure. Best-fit exponential curve with a R^2 value of 0.9816. (**e**,**f**) Norbornene−thiol reactions with different LAP or DMPA concentrations. (**g**,**h**) Norbornene-thiol reaction UV wavelengths of 365 nm or 390 nm wavelengths for LAP and DMPA photoinitiators.

employed for bioactive conjugations or cell encapsulation; however, there are limitations in the concentration and UV exposure times for both. The specific combinations of photoinitiator, concentration, and UV exposure required for successful retention of protein bioactivity and/or cell viability are depicted in Fig. 4.:2 mM LAP with 1−2 min UV or 2 mM DMPA with 1 min UV gives both excellent cell viability and protein bioactivity. Furthermore, Table 1 summarizes the different applications for photoinitiators LAP and DMPA.

3.3. Stiffness of acrylate and thiol-ene hydrogels

To begin comparing acrylate and thiol-ene hydrogels as cell culture substrates, we observed their mechanical properties. First, acrylate and thiol-ene hydrogels were synthesized via their respective reaction protocols (Fig. 5a). We modulated PEG reactant concentration within the precursor solution and measured the resulting hydrogel stiffness. Acrylate hydrogels were able to achieve different magnitudes of stiffness, ranging from 1 kPa to 100 kPa by altering the weight per volume solutions from 5 to 20% PEGDA (3.4 kDa), respectively (Fig. 5b). Thiol-ene hydrogels, however, exhibited a much smaller range in stiffness. Specifically, 8-arm norbornene PEG monomers (20 kDa) reacted with dithiol PEG monomers (3.4 kDa) at 5%, 10% and 20% concentrations resulted in hydrogel stiffness all less than 5 kPa (Fig. 5c). It is evident that acrylate hydrogels, without altering PEG monomer's molecular weight, can provide a wide range of stiffness. On the other hand, thiol-ene hydrogels are limited and only fine tuning stiffness properties can be established by modulating the PEG monomer concentration alone. To expand thiol-ene hydrogel stiffness range to different magnitude, it is expected that molecular weight of the PEG reactants needs to be manipulated.

Next, we evaluated UV exposure time effects on hydrogel stiffness. We noticed both acrylate and thiol-ene hydrogels were able to

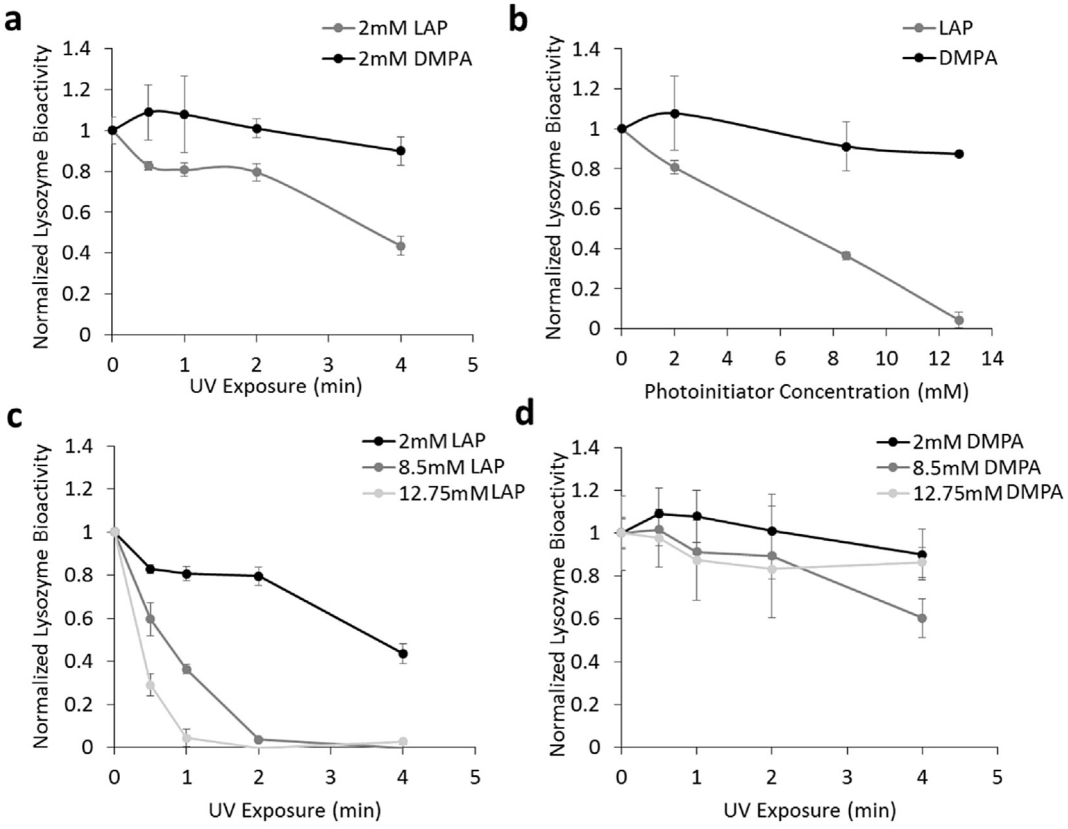

Fig. 2. Protein bioactivity response to photoinitiator and UV exposure. (**a**) LAP and DMPA at 2 mM concentration compared in protein bioactivity retention over 4 min of UV light (365 nm). (**b**) Protein bioactivity dependence on photoinitiator concentration for both LAP and DMPA. (**c,d**) Bioactivity for different concentrations of LAP and DMPA over 4 min of UV exposure.

create a gel around 1 min of UV exposure. Importantly, we found more UV exposure to acrylate hydrogels would continue to increase the stiffness (Fig. 5d). In contrast, thiol-ene hydrogels revealed no increase in stiffness with prolonged UV exposure (Fig. 5e). This data illustrates acrylate reactions are incomplete at 1 min of UV and will continue to react with additional UV exposure. Thiol-ene reactions, on the other hand, are completed at 1 min of UV and no further crosslinking occurs with additional exposure. This data further confirms reaction properties observed in kinetic reaction studies (Fig. 1), discussed in the previous section. Overall, both systems provide stiffness ranges that can successfully mimic a variety of tissues stiffness.

Modulation of substrate stiffness is one of the approaches to control cell behaviors such as morphology, migration, and certain stem cell fates [3,17,18]. As an example, we illustrate acrylate hydrogels at different stiffness can affect how differentiating stem cells attach and grow overtime (Fig. 5f–h). We observed mESCs differentiate on a soft hydrogel (5%PEG, 1 KPa) as a monolayer (Fig. 5f) whereas mESCs on a stiff hydrogel (20%PEG, 100 kPa) resulted in cell aggregates (Fig. 5h). Additionally, acrylate and norbornene hydrogels can be used to encapsulate cells in 3D (Supplemental Fig. S3) Different dimensionality cultures are commonly found in stem cell differentiation approaches. We illustrate that we can create different growth environments through simple manipulation of the precursor gel solution.

3.4. Surface patterning of acrylate and thiol-ene hydrogels

Both acrylate and thiol-ene PEG hydrogels are capable of spatial conjugation of thiolated proteins to their surface via thiol-ene reactions. In short, to pattern protein on acrylate gel, thiol modified proteins are spread across the hydrogel's surface evenly, a photomask is placed directly onto the surface and the gel is exposed to a second round of UV light. Unreacted proteins are washed away and patterned fluorescently tagged proteins can be observed using fluorescence microscopy.

Thiol-ene hydrogels require a more complex method for surface protein patterning (Fig. 6). As most norbornene groups are fully reacted due to the high efficiency of thiol-norbornene reaction during hydrogel forming process, this leaves very little free norbornene groups available for additional surface patterning with thiol-proteins. We have developed a protocol for robust surface bioconjugation on PEG-norbornene hydrogels. First, PEG-dithiol, 8-arm norbornene PEG, a photoinitiator, and an extracellular protein (*e.g.* fibronectin, laminin) are mixed and exposed to UV light (Fig. 6a). 8-arm norbornene PEG is the limiting reactant to provide complete crosslinking throughout the gel. From experimental values, we found that a molar ratio of 1:8 (8-arm norbornene PEG to PEG-dithiol) or higher allows for complete surface thiol saturation, suggesting a completed hydrogel network throughout (Fig. 6b). Next, a small volume of multi-arm norbornene PEG is spread onto the surface of the hydrogel and the gel is exposed to a second round of UV light (Fig. 6c). This will replace the saturated thiol surface with copious norbornene functional groups for targeted bioconjugation. After this step, thiolated proteins are spread across the surface evenly, a photomask is placed directly onto the surface and the gel is exposed to another round of UV light (Fig. 6d). As previously discussed, the additional rounds of UV exposure will not alter the underlying stiffness of the thiol-ene hydrogel. Finally, unreacted proteins are washed away and the immobilized protein

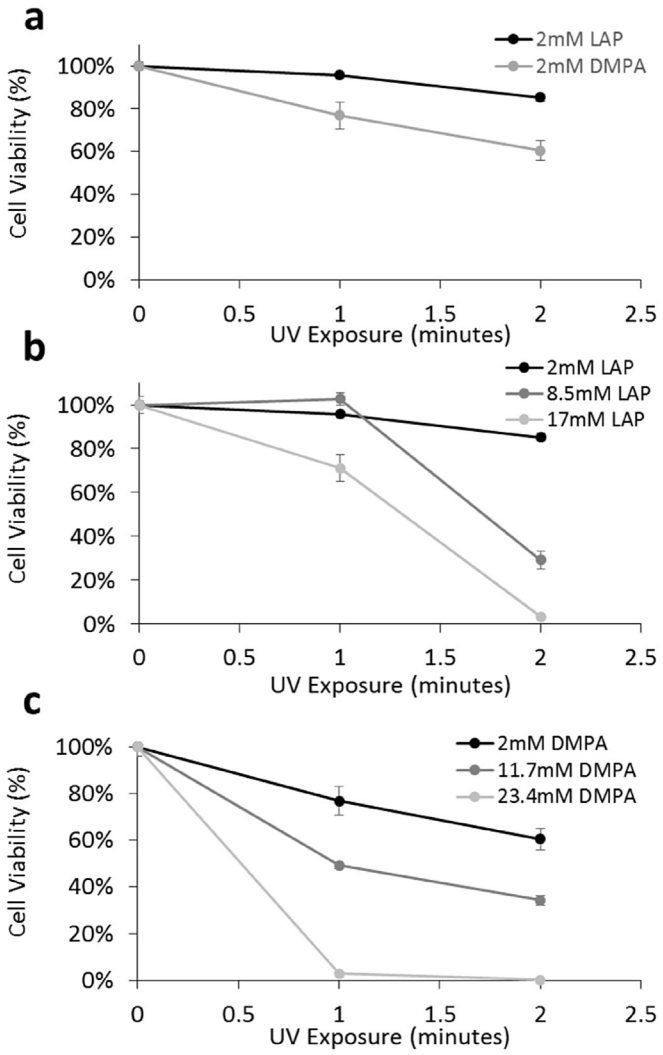

Fig. 3. Cell viability of HUVECs after exposure to photochemical treatments. (**a**) LAP and DMPA at 2 mM concentration compared in cell viability over 2 min of UV light (365 nm). (**b,c**) Cell viability for different concentrations of LAP and DMPA over 2 min of UV exposure.

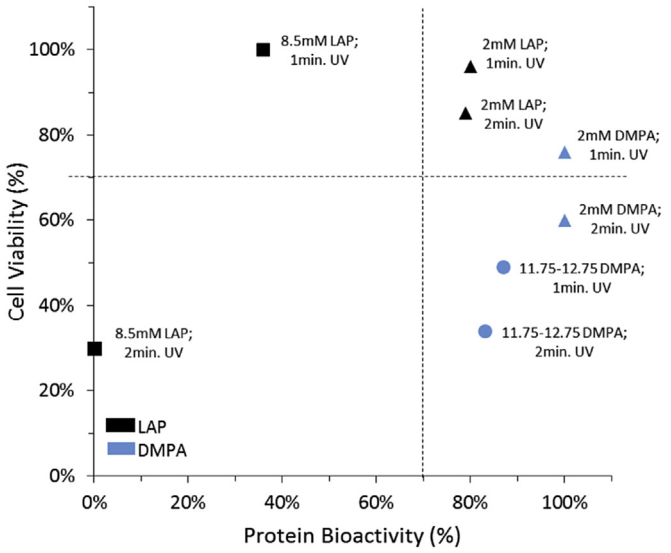

Fig. 4. Selecting photoreaction parameters for high cell viability and/or protein bioactivity. LAP (black) or DMPA (blue) photoinitiators at different concentrations and UV exposure times. Top right region parameters that can achieve both high cell viability (>705%) and bioactivity (>70%).

pattern remains (Fig. 6e).

To evaluate how patterning parameters contribute to the success of surface bioconjugation, we tested three key features for both hydrogel chemistries. First, we observed how UV exposure time of the protein pattern changes the amount of immobilized protein for both thiol-ene hydrogels and acrylate hydrogels. For both hydrogel systems, we found that increased UV exposure to the pattern resulted in more peptides conjugated to the surface, as expected (Fig. 7a). Specifically, pattern intensities increases with increased UV exposure (Fig. 7a). This property is of interest when looking to develop continuous protein gradients using UV light. Next, we investigated how UV exposure for hydrogel formation prior to patterning can affect the protein pattern. Here, we observed acrylate hydrogels had a significant loss of conjugated molecules when UV exposure times were greater than 2 min (Fig. 7b). In contrast, thiol-ene hydrogels depicted strong conjugated patterns independent of prior UV exposure times (Fig. 7b). This data highlights a key feature of our developed thiol-ene hydrogel platform compared to the acrylate system. That is, thiol-ene protocol relies solely on complete reactions for each synthesis step and therefore additional UV exposure does not effect the substrate's bioconjugation potential. However, acrylate hydrogels depends on residual acrylate groups remaining after an incomplete reaction of the hydrogel's network. Therefore, the more complete the hydrogel reaction is as time goes by, the less acrylate groups are available for bioconjugation on the surface and, thus, the amount of protein patterning is decreased. Finally, we tested how the concentration of thiolated molecules would influence the protein patterning strength. With both hydrogel systems, we noticed greater surface conjugation generated at higher peptide concentrations (Fig. 7c).

Both acrylate and thiol-ene hydrogels were successful substrates for creating immobilized protein patterns. Acrylate hydrogels require specific UV exposure times and therefore this platform is somewhat limited in its potential. Thiol-ene hydrogels, on the other hand, prove to have greater flexibility in its protocol parameters and shows promise for more complex bioactive systems.

3.5. Applications of bioactive hydrogel patterning

To highlight the potential of bioactive hydrogel patterns, we patterned VEGF onto PEG acrylate hydrogels. VEGF is a critical biochemical cue for angiogenesis and an important factor for *in vitro* culture of ECs. Additionally, VEGF is typically in ECM sequestration [19]. Therefore, to mimic this immobilized display of VEGF, we created VEGF patterned hydrogels and cultured HUVECs on these bioactive gels. We monitored EC response to the VEGF pattern over two days (Fig. 8). At first, ECs uniformly occupied the hydrogel's surface at initial cell seeding (Fig. 8a), but overtime HUVECs migrated towards the immobilized VEGF. After two days of culture, majority of ECs were observed on the VEGF pattern (Fig. 8b–c). VEGF patterned hydrogels remain bioactive for over two weeks when stored in 4 °C (Supplemental Fig. S4).

To illustrate another application for bioactive patterns, we developed a method for creating a continuous gradient. To achieve a gradient pattern, we modulated the UV exposure across the hydrogel's surface by using a programmable moving stage (Fig. 9a). At most, the hydrogel was exposed to 30 s of UV light and the opposite side received no UV exposure. This technique resulted in a continuous gradient (Fig. 9b–c). In this example, we patterned ephrinB2-Fc to study ephrinB2-EphB4 signaling in ECs. In general,

Table 1
Summary of photoinitiators and their usage.

	LAP	DMPA
Hydrogel/Bioconjugation Reactions	Thiol-ene Acrylate	Acrylate
UV Wavelengths	365 nm 390 nm	365 nm
Cell Encapsulation (HUVECs)	2 mM; 1min. UV (>95%) 2 mM; 2min. UV (>80%) 8.5 mM; 1min. UV (>95%)	2 mM; 1min. UV (>70%)
Bioactive Retention	2 mM; 1min. UV (>75%) 2 mM; 2min. UV (>75%)	2 mM; 1min. UV (>95%) 2 mM; 2min. UV (>95%) 12.75 mM; 1min. UV (>80%) 12.75 mM; 2min. UV (>80%)
Cell Encapsulation (>70%) and Bioactive Retention (>70%)	2 mM; 1min. UV 2 mM; 2min. UV	2 mM; 1min. UV

ephrins are membrane bound ligands that require cell-cell multivalent contact with membrane-bound Eph receptors for protein signaling. In the vascular system, ephrinB2 is uniquely express on arterial ECs and its receptor, EphB4, is express on vein ECs [20]. The signaling between ephrinB2 and EphB4 is known to play an important role in arterial venous vessel patterning [21]. To mimic this cell-cell signaling, immobilized gradient of ephrinB2-Fc was seeded with vein ECs (HUVECs), which express the EphB4 receptor. Shortly after cell seeding, HUVECs were attached uniformly across the hydrogel surface (Fig. 9d). Unlike VEGF pattern, overtime we observed HUVECs migrate away from immobilized ephrinB2-Fc. HUVECs on gradient ephrinB2 hydrogels at one, two and four days of culture (Fig. 9e–g). The ephrinB2 signal repels EphB4 expressing cells, suggesting this cell-cell signaling plays a role in the formation of arterial venous territory separations *in vivo*. These findings are supportive of others finding regarding ephrinB2-EphB4 signaling in the developing of arterial venous networks [21]. In summary, we were able to manipulate HUVECs to attract or repel in response to

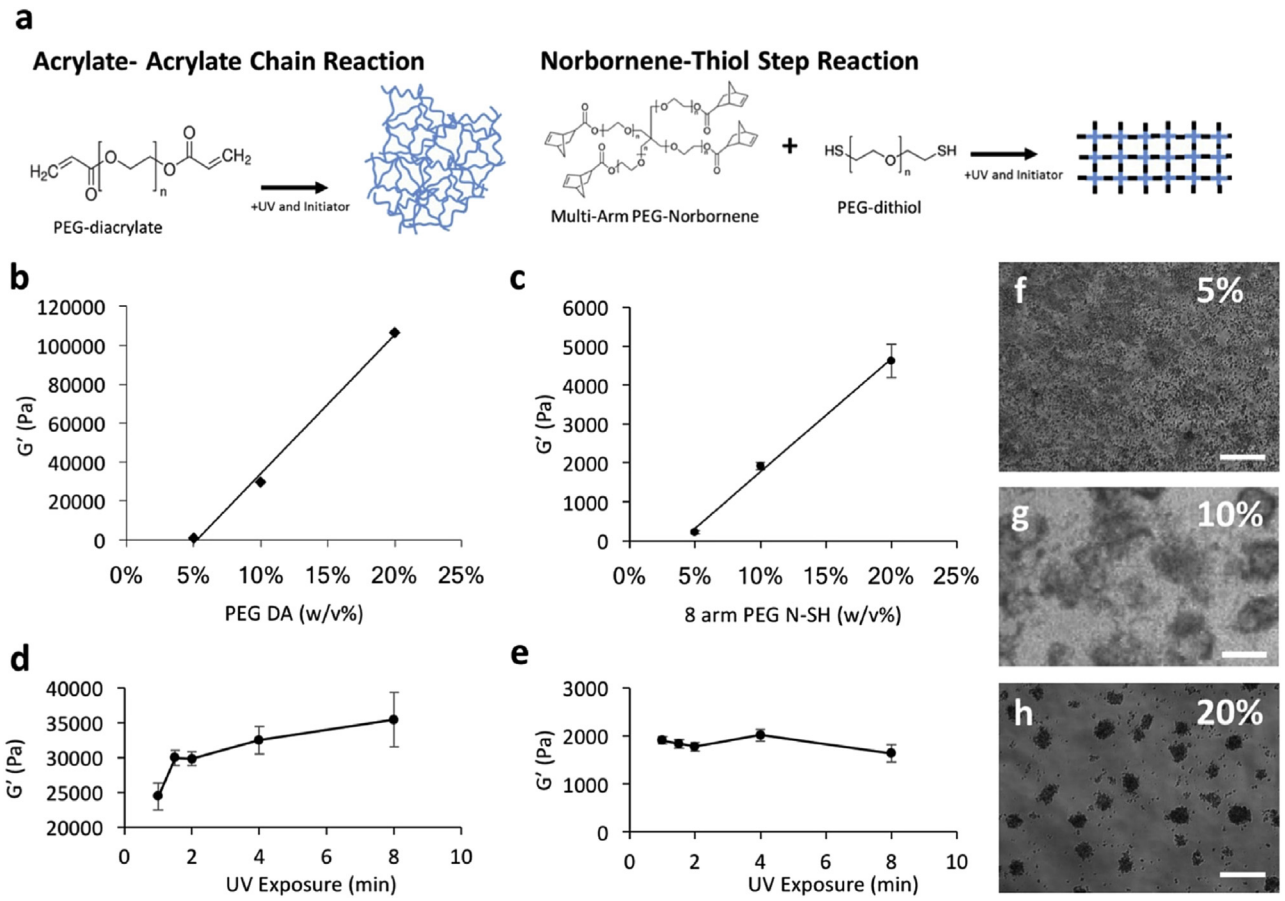

Fig. 5. Acrylate and thio-ene chemistry for hydrogel stiffness. (**a**) Schematics of acrylate hydrogel formation compared to norbornene thiol-ene hydrogel formation (**b,c**) Various percent PEG concentrations result in different hydrogel stiffness (G′) for **(b)** PEG acrylate (PEGDA) and **(c)** 8 arm PEG norbornene thiol-ene (8 arm PEG N-SH) hydrogels. (**d,e**) Hydrogel stiffness with increased UV exposure times for 10% (**d**) acrylate and (**e**) 8 arm norbornene thiol-ene hydrogels. (**f,g**) mESCs cultured on (**f**) 5%, (**g**) 10% or (**h**) 20% PEG acrylate hydrogels with fibronectin over three days in vascular differentiation media.

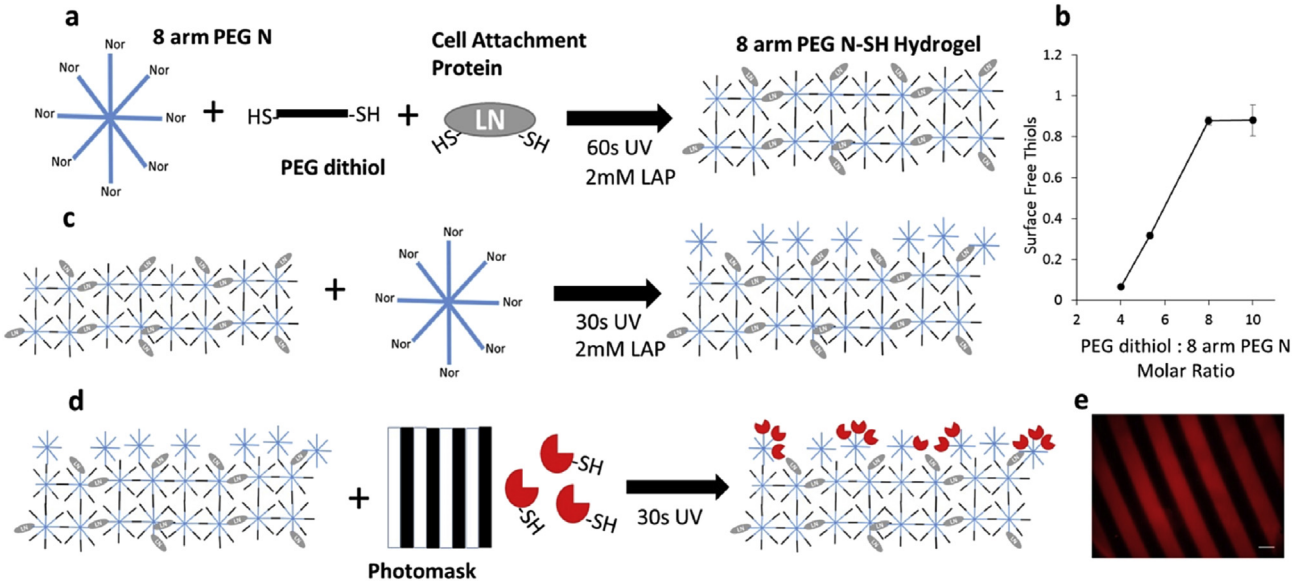

Fig. 6. Schematic for creating pattern using thiol-ene chemistry. (**a**) Hydrogel formation of 8 arm norbornene PEG (8 arm PEG N), dithiol PEG with thiolated ECM protein. (**b**) Measurement of surface free thiols after initial gel formation over various reactant molar ratios. (**c**) 8 arm PEG N reacted to thiol saturated hydrogel surface to replace free thiols with free norbornene for bioconjugation click reactions. (**d**) Photomask patterning of thiolated proteins to the surface. (**e**) Example of patterned thiol-ene hydrogel.

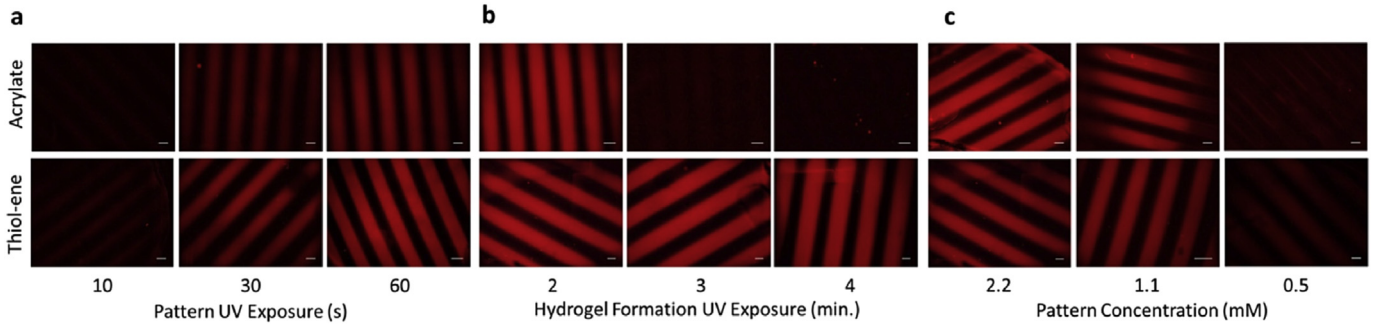

Fig. 7. Protein patterns on acrylate and thiol-ene hydrogels. (**a-c**) RGDC patterned on PEG diacrylate (top row) or 8 arm norbornene-thiol hydrogel (bottom row). (**a**) Pattern UV exposure for 10, 30 or 60 s. (**b**) Hydrogel UV exposure for 2, 3 or 4 min (**c**) RGDC concentrations of 2.2, 1.1 or 0.5 mM. Scale bars represent 200 μm.

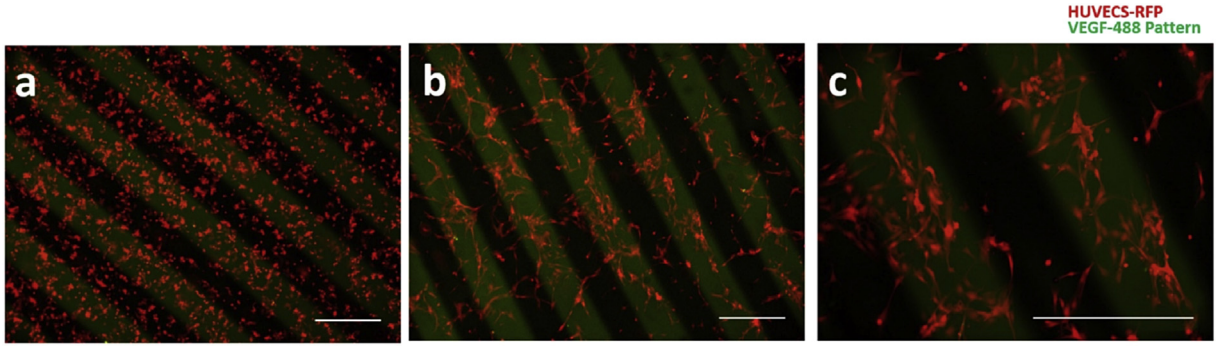

Fig. 8. VEGF patterns attract HUVECs. (**a-c**) HUVEC-RFP (red) seeded onto VEGF (green) patterned hydrogel images represent (**a**) 2 h (**b**) 8 h and (**c**) 24 h after cell seeding. Scale bar represents 500 μm.

different bioactive molecules and different spatial patterns. These examples add growing body of research illustrating the potential of ways to immobilize bioactive molecules to mimicry and study *in vivo* signaling that including sequestered growth factors [22–28], and cell-cell mimicry [12,29] and multivalent signals [30,31].

4. Conclusion

In this study, we investigated the role of photoinitiators and UV exposure with respect to acrylate and thiol-ene reaction kinetics, protein bioactivity, and cell viability. These parameters were

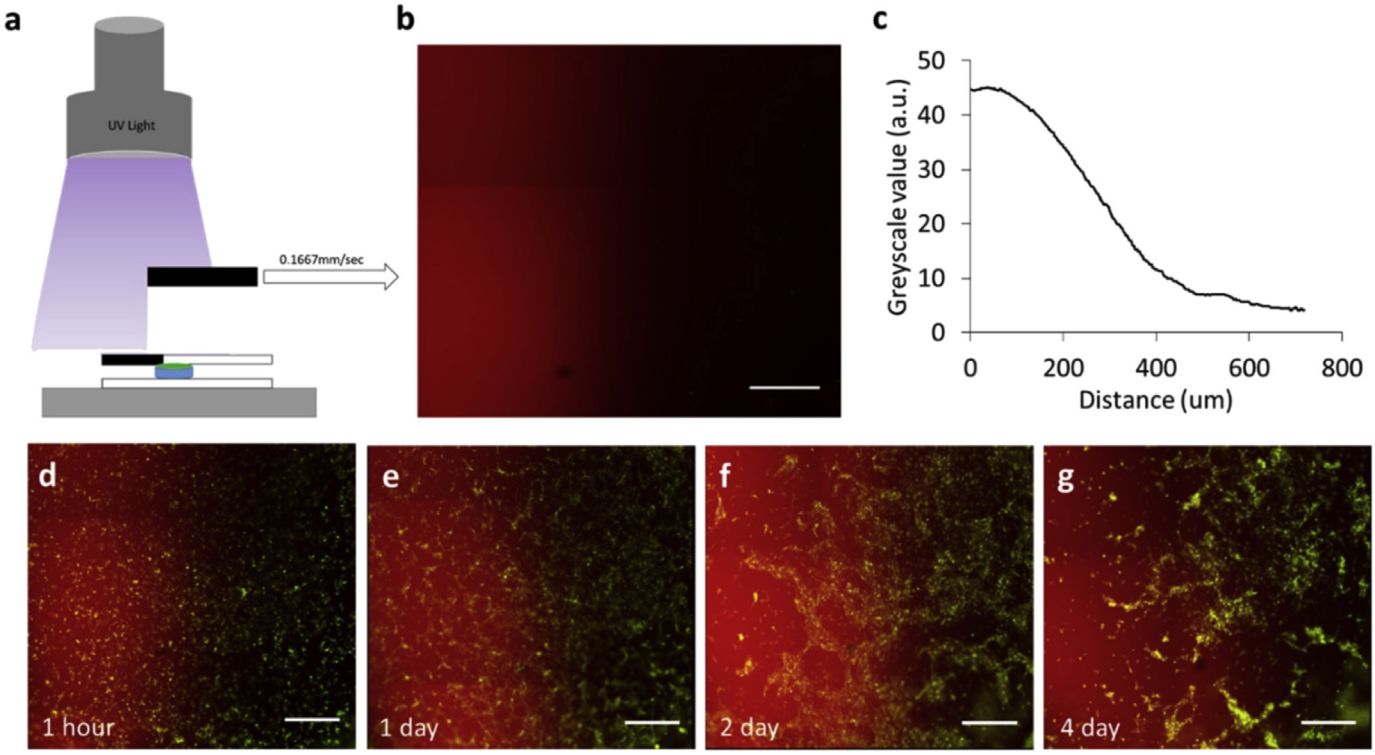

Fig. 9. EphrinB2-Fc gradient repel HUVECs. (**a**) Continuous gradient set up with programmable moving stage. (**b,c**) EphrinB2-Fc (red) gradient fluorescent image and associated greyscale values. (**d-g**) HUVECs-GFP (green) respond to gradient from (**d**) 1 h, (**e**) 1 day, (**f**) 2 days, and (**g**) 4 days post seeding. Scale bars represent 500 μm.

studied with the goal to develop a hydrogel system capable of bioactive conjugation, spatial patterning, cell encapsulation, and any combinations thereof. Our results highlight the photoinitiator type, concentration, and UV exposure times are important for different applications. We also evaluated acrylate and thiol-ene hydrogel systems for independently controlling substrate stiffness and surface protein patterning. Without changing monomer size, acrylate hydrogels can create large stiffness ranges with ease just by varying the hydrogel concentration, but needs carefully monitoring of the UV strength and time as the acrylate gel continues to change its stiffness with additional UV exposure. On the other hand, thiol-norbornene hydrogels demonstrate smaller stiffness ranges with regards to PEG-norbornene concentration and achieving large stiffness range requires modulating the molecular weight of PEG-norbornene monomer. Both hydrogel chemistries can be used for surface patterning and protein/peptide of interest, while PEG-norbornene has better independent control of stiffness and surface patterns. Moving forward, our developed patterning protocol for thiol-ene hydrogels illustrates parameter flexibility, better independent control of stiffness and surface patterning, and therefore is a superior candidate for more complex, multi-protein protein patterning. Overall, bioactive hydrogels have potential in extensive biological applications.

Acknowledgements

This study was supported mainly by grants from American Heart Association Scientist Development Grant (12SDG12050083 to G.D.), National Institutes of Health (R21HL102773, R01HL118245, R21HD090680 to G.D.) and National Science Foundation (CBET-1263455, CBET-1350240 to G.D.).

Appendix A. Supplementary data

Supplementary data related to this article can be found at http://dx.doi.org/10.1016/j.bioactmat.2017.05.005.

References

[1] D.E. Discher, P. Janmey, Y.L. Wang, Tissue cells feel and respond to the stiffness of their substrate, Sci. (New York, N.Y.) 310 (5751) (2005) 1139–1143.
[2] Shenglian Yao, Xi Liu, Shukui Yu, Xiumei Wang, Shuming Zhang, Qiong Wu, Xiaodan Sun, Haiquan Mao, Co-effects of matrix low elasticity and aligned topography on stem cell neurogenic differentiation and rapid neurite outgrowth, Nanoscale 8 (19) (2016) 10252–10265.
[3] N.D. Evans, C. Minelli, E. Gentleman, V. LaPointe, S.N. Patankar, M. Kallivretaki, X. Chen, C.J. Roberts, M.M. Stevens, Substrate stiffness affects early differentiation events in embryonic stem cells, Eur. Cells Mater. 18 (2009) 1–13 discussion 13-4.
[4] T. Yeung, P.C. Georges, L.A. Flanagan, B. Marg, M. Ortiz, M. Funaki, N. Zahir, W. Ming, V. Weaver, P.A. Janmey, Effects of substrate stiffness on cell morphology, cytoskeletal structure, and adhesion, Cell Motil. Cytoskelet. 60 (1) (2005) 24–34.
[5] Joseph P. Califano, Cynthia A. Reinhart-King, A balance of substrate mechanics and matrix chemistry regulates endothelial cell network assembly, Cell. Mol. Bioeng. 1 (2–3) (2008) 122–132.
[6] S. Ouasti, R. Donno, F. Cellesi, M.J. Sherratt, G. Terenghi, N. Tirelli, Network connectivity, mechanical properties and cell adhesion for hyaluronic acid/PEG hydrogels, Biomaterials 32 (27) (2011) 6456–6470.
[7] M.W. Tibbitt, K.S. Anseth, Hydrogels as extracellular matrix mimics for 3D cell culture, Biotechnol. Bioeng. 103 (4) (2009) 655–663.
[8] M.P. Lutolf, J.A. Hubbell, Synthetic biomaterials as instructive extracellular microenvironments for morphogenesis in tissue engineering, Nat. Biotechnol. 23 (1) (2005) 47–55.
[9] J. Zhu, Bioactive modification of poly(ethylene glycol) hydrogels for tissue engineering, Biomaterials 31 (17) (2010) 4639–4656.
[10] M.S. Hahn, L.J. Taite, J.J. Moon, M.C. Rowland, K.A. Ruffino, J.L. West, Photolithographic patterning of polyethylene glycol hydrogels, Biomaterials 27 (12) (2006) 2519–2524.
[11] J.D. McCall, K.S. Anseth, Thiol-ene photopolymerizations provide a facile method to encapsulate proteins and maintain their bioactivity,

Biomacromolecules 13 (8) (2012) 2410–2417.
[12] J.E. Saik, D.J. Gould, A.H. Keswani, M.E. Dickinson, J.L. West, Biomimetic hydrogels with immobilized ephrinA1 for therapeutic angiogenesis, Biomacromolecules 12 (7) (2011) 2715–2722.
[13] B.D. Fairbanks, M.P. Schwartz, C.N. Bowman, K.S. Anseth, Photoinitiated polymerization of PEG-diacrylate with lithium phenyl-2,4,6-trimethylbenzoylphosphinate: polymerization rate and cytocompatibility, Biomaterials 29 (2012) 997–1003.
[14] Benjamin D. Fairbanks, Michael P. Schwartz, Alexandra E. Halevi, Charles R. Nuttelman, Christopher N. Bowman, Kristi S. Anseth, A versatile synthetic extracellular matrix mimic via thiol-norbornene photopolymerization, Adv. Mater. 21 (48) (2009) 5005–5010.
[15] B.V. Sridhar, N.R. Doyle, M.A. Randolph, K.S. Anseth, Covalently tethered TGF-beta1 with encapsulated chondrocytes in a PEG hydrogel system enhances extracellular matrix production, J. Biomed. Mater. Res. A 102 (2014) 4464–4472.
[16] B.H. Northrop, R.N. Coffey, Thiol-ene click chemistry: computational and kinetic analysis of the influence of alkene functionality, J. Am. Chem. Soc. 134 (33) (2012) 13804–13817.
[17] M. Jaramillo, S.S. Singh, S. Velankar, P.N. Kumta, I. Banerjee, Inducing endoderm differentiation by modulating mechanical properties of soft substrates, J. Tissue Eng. Regen. Med. 9 (1) (2015) 1–12.
[18] K. Ye, X. Wang, L. Cao, S. Li, Z. Li, L. Yu, J. Ding, Matrix stiffness and nanoscale spatial organization of cell-adhesive ligands direct stem cell fate, Nano Lett. 15 (7) (2015) 4720–4729.
[19] D. Krilleke, A. DeErkenez, W. Schubert, I. Giri, G.S. Robinson, Y.S. Ng, D.T. Shima, Molecular mapping and functional characterization of the VEGF164 heparin-binding domain, J. Biol. Chem. 282 (38) (2007) 28045–28056.
[20] H.U. Wang, Z.F. Chen, D.J. Anderson, Molecular distinction and angiogenic interaction between embryonic arteries and veins revealed by ephrin-B2 and its receptor Eph-B4, Cell 93 (5) (1998) 741–753.
[21] T. Füller, T. Korff, A. Kilian, G. Dandekar, H.G. Augustin, Forward EphB4 signaling in endothelial cells controls cellular repulsion and segregation from ephrinB2 positive cells, J. Cell Sci. 116 (Pt 12) (2003) 2461–2470.
[22] M. Nakajima, T. Ishimuro, K. Kato, I.K. Ko, I. Hirata, Y. Arima, H. Iwata, Combinatorial protein display for the cell-based screening of biomaterials that direct neural stem cell differentiation, Biomaterials 28 (6) (2007) 1048–1060.
[23] J.C. Igwe, P.E. Mikael, S.P. Nukavarapu, Design, fabrication and in vitro evaluation of a novel polymer-hydrogel hybrid scaffold for bone tissue engineering, J. Tissue Eng. Regen. Med. 8 (2) (2014) 131–142.
[24] Gina M. Policastro, Fei Lin, Laura A. Smith Callahan, Andrew Esterle, Matthew Graham, Kimberly Sloan Stakleff, Matthew L. Becker, OGP functionalized phenylalanine-based poly(ester urea) for enhancing osteoinductive potential of human mesenchymal stem cells, Biomacromolecules 16 (4) (2015) 1358–1371.
[25] V.H. Fan, K. Tamama, A. Au, R. Littrell, L.B. Richardson, J.W. Wright, A. Wells, L.G. Griffith, Tethered epidermal growth factor provides a survival advantage to mesenchymal stem cells, Stem Cells Dayt. Ohio 25 (5) (2007) 1241–1251.
[26] L.M. Alvarez, J.J. Rivera, L. Stockdale, S. Saini, R.T. Lee, L.G. Griffith, Tethering of epidermal growth factor (EGF) to beta tricalcium phosphate (βTCP) via fusion to a high affinity, multimeric βTCP-binding peptide: effects on Human multipotent stromal cells/connective tissue progenitors, PLoS One 10 (2015) 1–21.
[27] M. Rodrigues, Surface tethered epidermal growth factor protects proliferating and differentiating multipotential stromal cells from FasL induced apoptosis, Stem Cells 31 (2013) 104–116.
[28] P.R. Kuhl, L.G. Griffith-Cima, Tethered epidermal growth factor as a paradigm for growth factor-induced stimulation from the solid phase, Nat. Med. 2 (9) (1996) 1022–1027.
[29] C. Lin, K.S. Anseth, Cell – cell communication mimicry with poly (ethylene glycol) hydrogels for enhancing β-cell function, Natl. Acad. Sci. 108 (2011) 1–6.
[30] T. Vazin, R.S. Ashton, A. Conway, N.A. Rode, S.M. Lee, V. Bravo, K.E. Healy, R.S. Kane, D.V. Schaffer, The effect of multivalent Sonic hedgehog on differentiation of human embryonic stem cells into dopaminergic and GABAergic neurons, Biomaterials 35 (3) (2014) 941–948.
[31] A. Conway, T. Vazin, D.P. Spelke, N.A. Rode, K.E. Healy, R.S. Kane, D.V. Schaffer, Multivalent ligands control stem cell behaviour in vitro and in vivo, Nat. Nanotechnol. 8 (11) (2013) 831–838.